Spy1-activated Cyclin Dependent Kinase 2 Shows Reduced Affinity for Current Synthetic Small Molecule Inhibitors of the CDK2-Cyclin Complex

Daniel Meister[a], John J. Hayward[a], Bre-Anne Fifield[b], Lisa A. Porter*[b], John F. Trant*[a]

[a]Department of Chemistry and Biochemistry, University of Windsor, Windsor, ON N9B 3P4, Canada; [b]Department of Biomedical Sciences, University of Windsor, Windsor, ON N9B 3P4, Canada

Corresponding Authors: lporter@uwindsor.ca; jtrant@uwindsor.ca

Abstract: Cyclin-dependent kinases (CDKs) play a key role in activating essential cell biology processes including cellular proliferation. Inappropriate regulation of CDKs has been implicated in driving several different forms of cancer. One of the regulatory factors is the need to bind to Cyclin-partners before they can be activated and advance the cell cycle. Cyclins are overexpressed in several different cancers, hence activating their relevant CDK. Hyperactive CDK2 in particular is implicated in many cancers, and while many drugs have shown preclinical promise, none have successfully passed through clinical development. Among the complications of targeting CDK2 is the fact that non-classical cyclin partners from the Speedy/RINGO family of proteins can alter the conformation of the kinase. Using computational approaches, we provide data supporting that the active site of CDK2 differs when bound to Spy1 as compared to classical cyclins. Furthermore, combining computational models with experimental techniques we provide data that many small molecule inhibitors have reduced activity against Spy1-bound CDKs. This work supports the need to develop new inhibitors capable of inhibiting the Spy1-CDK2 complex, and suggests that computational tools can be beneficial toward accomplishing this goal.

Introduction

Carefully timed post-translational modification of enzymes in the Cyclin-Dependent Kinase (CDK) family control serine/threonine phosphorylation that subsequently dictates how cells move through the phases of the cell cycle.[1] Several independently regulated events are required for CDK activation, including binding to their regulatory cyclin partner and alterations in phosphorylation status, to ultimately provide substrates access to the kinase active site.[2] Each CDK has preferred cyclin partners—for example, CDK2 is activated by either Cyclin A or E; cyclin proteins are themselves regulated *via* protein expression and degradation. The binary "on" Cyclin-CDK complex can be turned "off" by binding to naturally occurring inhibitory proteins (CDK inhibitors: CKIs), which sterically block substrate access to the kinase active site.[3] Inhibition, deactivation, and degradation of CDKs is essential to maintain proper cell growth in healthy normal tissue. On the other hand, sustained activation of Cyclin-CDK complexes are at the heart of disease states such as cancer.[4] Restoring the inhibition of CDK proteins is a promising anticancer therapeutic strategy,[5] with the G1/S CDK, CDK2, being one prominent target.[6] Unlike the G2 CDK (CDK1), inhibition of CDK2 *via* chemical inhibition, or knockout/knockdown approaches is not lethal for the organism as CDK2 is not essential for the viability and division of most normal cell types.[7] Synthetic lethality of select forms of cancer however has been reported.[8] Despite the promise of this approach, the development of synthetic CKIs has proven challenging: ATP-competitive inhibitors are an effective approach, however selectivity is often an issue as the enzyme active site is highly conserved across the CDK family and highly analogous to unrelated proteins that also interact with ATP. This can lead to many off-target effects, and first generation pan-CKIs failed due to lack of selectivity, with inevitable high toxicity.[9] Second generation inhibitors were more selective against specific CDK targets, reducing their toxicity. CKIs targeting

CDK4 and CDK6 have been approved as a standard of care therapy in the treatment of hormone receptor-positive, HER2-negative breast cancer.[10] No CDK2 inhibitor has obtained regulatory approval for standard of care treatment.

This dearth of CDK2 inhibitors approved for treatment is despite many molecules having shown good binding affinity and good activity *in vitro* and *in vivo* in animal model systems.[9] An overlooked factor that may have contributed to these translational failures around CDK2 is the existence of the "cyclin-like" proteins, known as the Speedy/RINGO family. The original characterized member of this family, Spy1, binds CDK1 and CDK2 in the absence of classical cyclins and is insensitive to inhibition by endogenous CKIs such as p21 and p27; Spy1 actually targets p27 for degradation.[11] The Spy1-CDK2 complex is activated irrespective of the post-translational modifications required for full activation of Cyclin-CDK complexes.[12] Consequently, Spy1 binding results in a perpetually active CDK, leaving the CDK in a locked "on" position, helping to accelerate cells through the cell cycle, and driving cellular proliferation.[12] Spy1 is found at only very low levels in most adult tissue, with the exception of select stem cell populations, transient developmental timepoints and transiently expressed during stress or regenerative responses, where expression is related to overriding cell cycle checkpoints.[13] Unsurprisingly, the sustained elevation of Spy1 in mouse models results in susceptibility to tumourigenesis in a variety of systems including breast and liver.[14] The overexpression of Spy1 has been implicated in numerous aggressive forms of cancer including breast, prostate, ovarian, liver and brain, with levels positively correlating with poor prognosis.[14-15] One reason for these poor outcomes is that Spy1 overexpression is also positively correlated with drug resistance; for example, chemotherapy drugs and tamoxifen are significantly less effective when Spy1 is overexpressed.[16] Given the

ability of Spy1 to drive drug resistance and the insensitivity to endogenous CKIs, this could potentially be why development of CDK2 inhibitors has been unsuccessful.

Therapeutic synthesis has focused upon the canonical Cyclin-CDK complexes and has failed to account for CDK activation by Spy1. The Spy1-CDK2 crystal structure[12] suggests that the binding pocket of Spy1 may differ from that of Cyclin A-CDK2 which could alter the binding affinity of CKIs and contribute toward clinical failure in patients with cancers with elevated Spy1 levels. This idea supports the potential opportunity to develop novel more effective compounds. Knockout of Spy1 in mice renders them sterile due to an essential role in meiosis, but seems to have no other detrimental effects.[17] In fact, Spy1 inhibitors have been proposed as potentially effective and safe male birth control agents.[18] This safety profile, when combined with the altered binding site, suggests that new selective CKIs targeting the Spy1-CDK complex could prove useful cancer therapies that address this potential mechanism of failure of previous generations of CDK inhibitors.

In this study we aimed to determine whether elevated Spy1 levels contribute to the ineffectiveness of established leading small molecule CKIs for CDK2 using a combined computational and experimental approaches. We focused both on commercially available 2nd generation CKIs,[19] and on a promising series of N2 and O6 substituted guanine derivatives, developed first by the Golding and Griffin groups at Newcastle University and referred to as the NU series of compounds (**Figure 1**).[19a, b, 20] We synthesized several of these NU compounds to determine their *in vitro* efficacy in the presence of over-expressed Spy1. Computational data revealed that CKI binding affinity in these molecules for the Spy1-CDK2 complex is significantly reduced compared to their potent activity against CyclinA/E-CDK2. This was supported by the

experimental data and the compounds are ineffective in inhibiting cell proliferation *in vitro* when Spy1 is present.
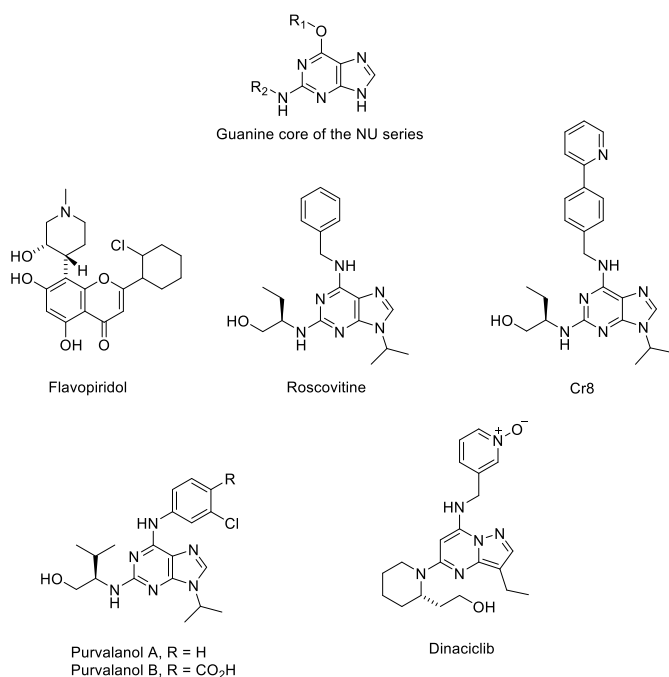

Figure 1 Structures of examined CKIs.

Experimental and Computational Methods

Computational Methods

Structure preparation: Protein crystal structures of active (*i.e.* phosphorylated) Cyclin A-CDK2 with no ligand (PDB: *1JST*)[21], Cyclin A-CDK2 with bound inhibitor NU6102 (*1H1S*)[20c] and Spy1-CDK2 (*5UQ1*)[12], Cyclin E-CDK2 (*5L2W*)[22] and Cyclin B-CDK1 (*5LQF*)[19d] were obtained from the Protein Data Bank.[23] Solvent molecules were deleted, and the structures were prepared using the protein preparation wizard module in the Schrödinger computational suite; missing loops were added.[24] The pH was set to 7 and the prepared structures were then minimized. A second model was also generated from *1JST*, conserving some active site water molecules to

determine if they were important for binding. Other complexes had solvent molecules removed as they were found to not have any impact on the docking following some preliminary scoping investigations. Ligand structures were prepared using Ligprep in Schrödinger.[25] A total of 79 NU series ligands were screened alongside 6 commercial CKIs: CR8, dinaciclib, flavopiridol, purvalanol A, purvalanol B, and roscovitine (**Figure , Table S1**).

Docking Study: Both rigid and induced fit docking was performed. Rigid docking was performed using GlideXP in Schrödinger with enhanced sampling and induced fit was performed using extended sampling.[26] Several receptor grids were generated with different van der Waals (vdW) radius scaling and with flexible hydroxyl groups. During initial rigid docking, several compounds (known binders) failed to bind due to the constricted active sites and lack of flexibility in rigid docking. Thus, two models with scaled vdW radii were generated, 1.0 (default) and 0.7 radii. MM-GBSA in Schrödinger was performed using the top pose for each compound, with 8 Å of flexibility around the ligand. The VSGB solvation model[27] and OPLS4[28] forcefield were used.

Molecular Dynamics: Molecular dynamics simulations were performed using AMBER20.[29] Three different methods, RESP (Restrained ElectroStatic Potential), Gasteiger, and AM1-BCC were tested for parameterizing ligands and generating partial atomic charges. This was done to obtain the best method for further screening of new compounds. Traditionally RESP is used to generate ligand charges;[30] ligands were optimized using the HF/6-31G* level of theory in the gas phase in Gaussian16.[31] Gasteiger and AM1-BCC charges were generated using Antechamber in AmberTools.[32] Gasteiger charges are computationally less expensive to generate and are based on atom types and connectivity. Several studies reported that they yield better results when calculating small molecule binding affinity.[33] AM1-BCC is a semi-empirical method and is

faster and easier to implement than RESP. AM1-BCC has been reported to having similar results to RESP methodology.[33-34]

Parameters for small molecules were produced using the general AMBER force field (GAFF),[35] while ff14SB[36] was used for the protein, and TIP3P[37] for water molecules. Complexes were placed in a 12 Å isometric water box. Sodium or chloride ions were added to neutralize the system. The system was minimized over three steps with decreasing restraints of 100, 3, and 0 kcal·mol^{-1}·Å^{-2}, with 10,000 steps steepest decent followed by 10,000 steps conjugate gradient. This was followed by heating to 300 K over 50 ps and then density equilibration for 250 ps. All simulations were performed using the NPT ensemble with periodic conditions with a temperature of 300 K using the Langevin thermostat. The system was then equilibrated for 4 ns followed by a 10 ns production run on which the MM-GBSA calculations are performed, and simulations were performed in triplicate and average binding affinity values taken.

MM-GB(PB)SA calculations: Binding free energy calculations were performed using MMPBSA.py.MPI in AMBER employing the SANDER module. An ionic strength of 0.1M was used and both MM-GBSA and MM-PBSA calculations were performed sampling every 1 ps from the production run. Two solvation models were tested (GB-Neck2 and OBC-2) and both yielded similar results.

Experimental Methods

Cell Culture: MDA-MB-231 (HTB-26; ATCC) and MDA-MB-468 (HTB-132; ATCC) were cultured in Dulbecco's modified Eagle's medium (DMEM; D5796; Sigma Aldrich) supplemented with 10% foetal bovine serum (FBS; F1051; Sigma Aldrich) and 1% P/S. and

maintained at 5% CO_2 at 37°C. For CKI treatment, cells were seeded in 24 well tissue culture plates at a density of 20,000 cells per well. CKIs were added 24hrs post-seeding and cell viability was assessed *via* trypan blue exclusion using a BioRad TC10 Automated Cell Counter. Cells were treated with reported and experimentally determined IC50s for each compound tested as indicated: 71.34nM CR8, 73.88nM flavopiridol, 10.18nM dinaciclib, 20μM roscovitine, 30μM purvalanol A, 640μM NU series compounds 4, 320μM NU series compound 6 and 8μM for NU series compounds 12, 14, 15.

Results and Discussion

Therapeutic synthesis has focused upon the canonical Cyclin-CDK complexes and has failed to account for CDK activation by Spy1. This would not matter if the CDK2 active site was the same whether a classical cyclin or Spy1 was bound; optimization of a drug for one would work for both; however, a comparison of the recently obtained Spy1-CDK2 crystal structure[12] with that of Cyclin A-CDK2 shows that the G-loop which sits atop the ATP binding site, the target of synthetic CKI drugs, is twisted by Spy1 binding. In both the crystal structure, and in all MD simulations, The tyrosine, which normally sits outside the binding pocket, being folded inwards and sitting on top of the binding site, resulting in a more constrained and hydrophobic pocket (**Figure**). This result supports that the altered binding site could reduce the binding affinity of CKIs resulting in decreased efficacy supporting the need to model the interaction of existing CKIs with Spy1-bound CDK2.
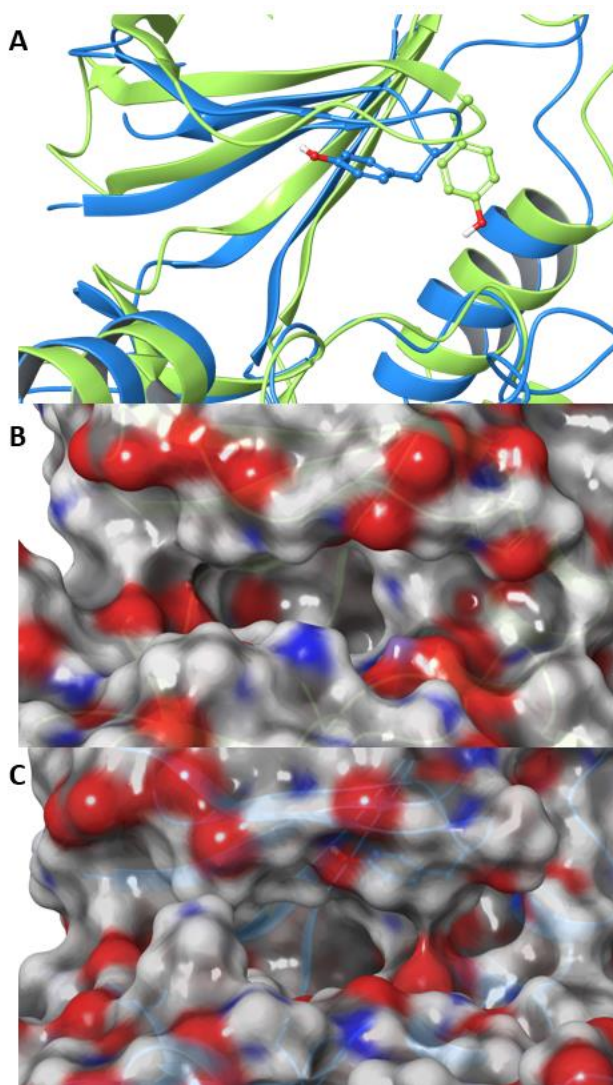
Figure 2 A) Orientation of the G-loop and tyrosine position in Cyclin A-CDK2 crystal structure (Green, PDB: 1JST) and Spy1-CDK2 (Blue, PDB: 5UQ1). B) Molecular surface of the Cyclin A-CDK2 binding site and C) Spy1-CDK2 showing the smaller more constrained site.

Initially, several docking parameters were tested to determine the ideal parameters and validate our approach. To determine if any protein model and docking protocol is appropriate for a given problem, the model must be evaluated against a self-consistent and well-conducted experimental dataset. As the NU series has the most data for CDK2 binding— and was performed by a single group with consistent and strong methodology— this set was used to benchmark the docking. The relaxed structure of active Cyclin A-CDK2 with bound NU6102 (PDB: *1H1S*)[20c] was

used as the receptor to validate the docking. The vdW radii of the receptor grid was scaled down slightly to 0.7 as some of the larger ligands, confirmed *in vitro* hits, failed to dock during the initial round of docking which used the 1.0 (default) value. Overall, a good correlation was obtained with experimental data (**Figure 3A**). Comparison of the docking poses of NU6102 to the crystal structure showed we could recapitulate the binding as the second-best pose had an RMSD of 0.29 Å, with the top pose having an RMSD of 1.01 Å. This slight difference is due to the top pose having a small shift in the cyclohexyl ring which was predicted as being more favourable (**Figure 4A**). The docking scores, however, were nearly identical with only a 0.02 kcal/mol difference.
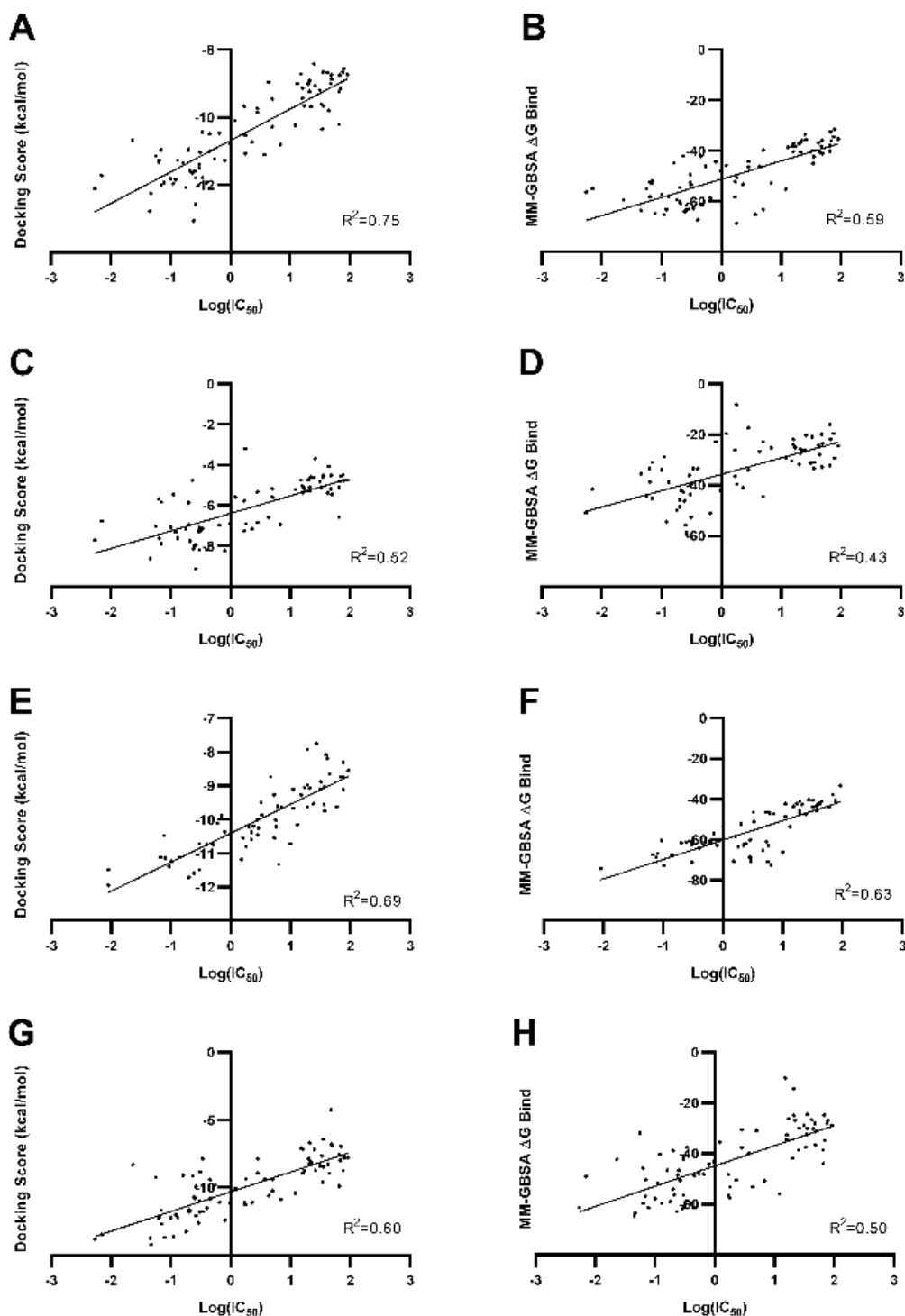
Figure 1 Comparison of docking scores (RRD or IFD) and MM-GBSA calculated scores (kcal/mol) to experimental IC_{50} values of the NU series binding to Cyclin A-CDK2. **A)** RRD using *1H1S* crystal structure as the template. **B)** MM-GBSA calculated binding affinities for *1H1S* as the receptor structure. **C)** RRD using *1JST* as the template structure. **D)** MM-GBSA calculated binding affinities using *1JST* as the receptor. **E)** RRD to Cyclin B-CDK1 (*5LQF*). **F)** MM-GBSA calculated binding affinities for Cyclin B-CDK1, *5LQF*. **G)** IFD of NU series to Cyclin A-CDK2(*1H1S*). **H)** MM-GBSA calculated binding affinities for Cyclin A-CDK2 (*1H1S*) based on IFD.

The pose observed in the crystal structure is potentially an artifact of better packing that aids its crystallization. The core of the rest of the ligands adopted similar conformations to that of NU6102 in the crystal structure with the core forming conserved hydrogen bonds with the backbone atoms of E81 and L83 of CDK2 (**Figure 4B**).
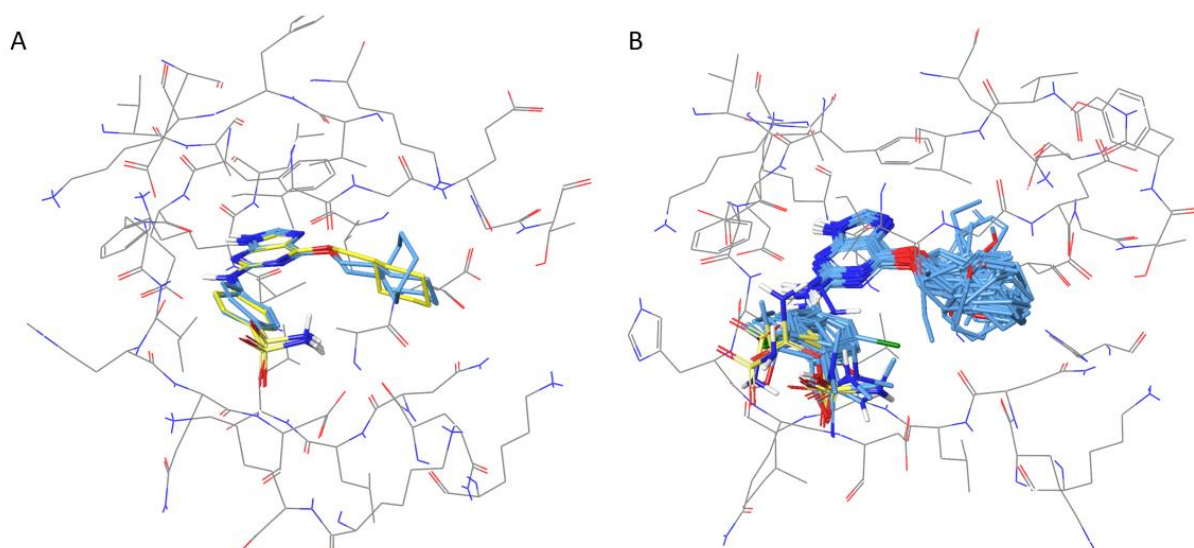
Figure 2 A) Overlay of top two docking poses of NU6102 docked to Cyclin A-CDK2(blue) and orientation of the ligand in the crystal structure (yellow). B) Alignment of the top docked pose of the NU series of compounds.

Docking to the crystal structure without a bound co-crystallized ligand (PDB: *1JST*)[38] yielded significantly worse results with $R^2=0.51$ (**Figure 3C**). With a bound ligand, the active site contracts, becoming much smaller to facilitate the ligand forming closer, more beneficial ligand-receptor contacts. This of course can be modelled using molecular dynamics simulations on docked structures and is feasible in this case, but this is a computationally expensive workflow for screening molecules on scale. Calculating binding affinity using the MM-GBSA module in Schrödinger, which allows nearby residues to move, did not improve the correlation ($R^2=0.43$), potentially because there was not enough flexibility to reorient the pocket to the degree that is observed in the bound form. Additionally, the presence of active site water molecules only had a

marginal effect on binding scores and based on the crystal structures with NU compounds bound, the majority of solvent molecules are displaced upon binding, and none of the remaining seeming to form any essential interactions. While the structure of Spy1-CDK2 already has a smaller, more constrained active site, leaving less room for contraction, these results indicate that molecular dynamics simulations would potentially be required to allow the pocket to rearrange and accommodate the bound ligands to obtain more accurate binding affinities. Induced fit docking (IFD) was also performed as it often yields significant improvements. In this case however, many of the compounds failed to bind in the orientation observed in crystal structures and resulted in significantly reduced predicted binding with an overall correlation of R^2=0.6. The MM-GBSA module of Schrödinger was also tested which allows for active site flexibility, which could potentially improve correlation. However, in all cases it performed more poorly than docking alone (**Figure 3B, D,F,H**).

Compounds were also docked to Cyclin B-CDK1. CDK2 and CDK1 share considerable homology. As a result, inhibitors will often bind to both complexes with similar affinities, and binding affinity data is available for most NU series compounds binding to Cyclin B-CDK1. Similar correlation values were obtained between docking score and experimental values (R^2=0.69, **Figure 3A**) as with the Cyclin A-CDK2 complexes.

It has been a long-standing goal to develop selective CDK2 inhibitors to minimize off-target effects; however, realizing this goal has proved to be challenging.[4b] This can be observed in the docking results where many of the compounds are predicted to have similar binding affinities to both complexes (**Table 1**). To better delineate the challenge, these inhibitors were also docked to Cyclin E-CDK2. Cyclin E also activates CDK2 and functions similarly to Cyclin A. While there is no experimental data to correlate to, it is important to know how well the compounds bind as

Cyclin E-CDK2 complexes still play an important role in cell cycle regulation. This would allow for comparison of CKIs across the different CDK complexes for a better understanding of their lack of selectivity and could be a useful prescreening tool for the development of future CKIs.

Comparison of docking scores across all complexes showed that the CKIs had the best binding to Cyclin A-CDK2, followed by Cyclin B-CDK1 and then Cyclin E-CDK2, with average binding being similar. Note that the identity of the cyclin was more important than the actual identity of the CDK that is being targeted. This highlights the challenge inherent in this drug discovery endeavour. However, the real insight from this study is that the ligands' affinity for Spy1-CDK2 was significantly worse than for any other complex (**Figure 5, Table S1**). This is likely due to the change in active site conformation in the Spy1-CDK2 complex. The inverted Y15 makes the pocket both more hydrophobic and smaller, resulting in more steric clashes as the alkyl/cyclohexyl moiety on many of the structures is forced into a less optimal position. This was also observed in commercially available CKIs (**Table 1**). Docking these CKIs to Cyclin A-CDK2 generated poses nearly identical to those observed in reported crystal structures; however, docking to Spy1-CDK2 yielded significantly different orientations and lower predicted binding as a result of the restricted active site not being able to accommodate the CKIs in the same conformations.

Table 1 Comparison of docking scores (kcal/mol) of commercial CKIs

	Flavopiridol	Roscovitine	Cr8	Purvalanol A	Purvalanol B	Dinaciclib
Cyc A-CDK2	−10.95	−9.61	−9.86	−10.53	−10.13	−12.43
Spy1-CDK2	−8.76	−6.47	−6.90	−6.54	−5.41	−8.78

Following rigid docking, the top pose, lowest energy conformation, for each ligand was selected and MD simulations were performed. Several parameters were tested to determine the optimal method. First, three different partial charge derivation methods were tested: RESP, AM1-BCC and Gasteiger (**Table 2**). All three have been successful when applied to small molecule protein-ligand binding; however, some differences are observed on a case-by-case basis and thus the best approach for a given system must be determined empirically.[33] RESP requires the use of Gaussian, while AM1-BCC and Gasteiger charges can be generated using tools built into AMBER (antechamber), with the latter two being significantly faster to perform; this is beneficial for compound screening. MM-GBSA calculations were then performed using an ion concentration of 0.1 M and the default solvation model. Both RESP and AM1-BCC performed reasonably well and yielded similar results with correlations of 0.76 and 0.71 respectively. However, Gasteiger charges performed significantly worse with a correlation of 0.24.
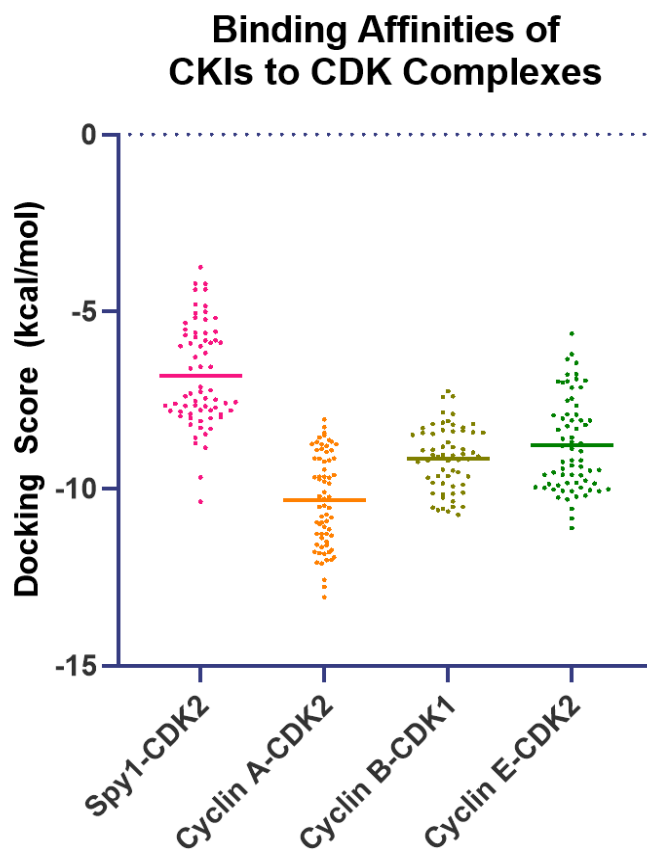
Figure 3 Comparison of docking scores of NU inhibitors across Cyclin-CDK complexes. Bars represent the mean binding affinity.

MM-PBSA energy calculations were also tested and compared to the MM-GBSA values. A correlation of 0.72 was obtained, but as MM-PBSA calculations generally take significantly longer than MM-GBSA calculations, and they did not offer an improvement, subsequent binding affinity calculations were performed using only MM-GBSA. Also tested were implicit generalized Born solvation models OBC-2 (igb=5 in AMBER) and the GB-Neck2 model (igb=8 in AMBER). GB-Neck2 offers some empirical corrections over OBC-2 model, however both performed similarly (**Table 2**), and the default, computationally less expensive OBC-2 model was used for the remaining calculations.

Table 2 Comparison of MD and MM-PB(GB)SA parameters.

		Correlation Coefficient
Partial charge method	RESP	0.73
	AM1-BCC	0.71
	Gasteiger	0.24
Solvation	IGB 5	0.76
	IGB 8	0.74
Binding Affinity Method	GBSA	0.71
	PBSA	0.72

The molecular dynamics simulations using RESP and OBC-2, were performed in triplicate for each system to better sample conformational space of the ligand and the obtained binding affinity used was the average of the three independent simulations. Overall, the docking scores and MM-GBSA results showed similar correlations. The binding affinities of the Spy1-CDK2 complexes were similarly calculated. Results showed that in nearly every case, the predicted binding affinities of the ligands binding to Spy1-CDK2 were worse than for Cyclin A-CDK2, reaffirming the results obtained during docking (**Figure 6**). While not tested for, the smaller more constrained active site of the Spy1-CDK2 complex may also inhibit ligand entry into the pocket in the first place, further reducing the ability of ligands to bind and their resulting efficacy.
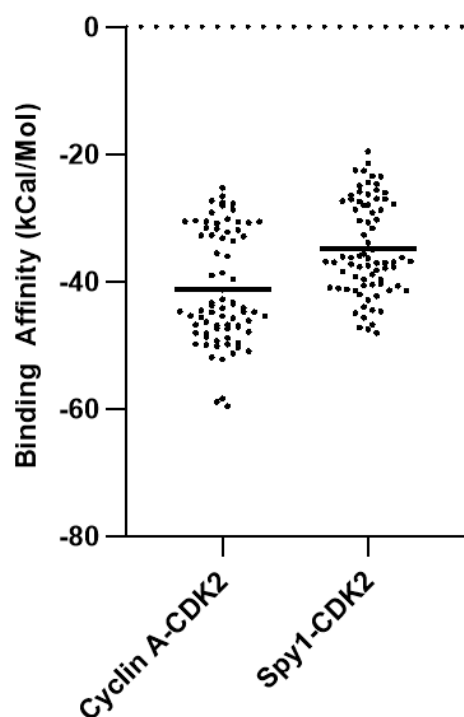
Figure 4 Binding affinity obtained from MM-GBSA calculations following MD simulations with bars representing mean binding affinity.

To determine if the observed reduced binding affinity to Spy1-CDK2 *versus* Cyclin A-CDK2 correlated with a reduction in cellular response, Spy1, Cyclin A and Cyclin E were overexpressed in the triple negative breast cancer cell lines MDA-MB-231 and MDA-MB-468. Cells were treated with a panel of CKIs and the total number of live cells was assessed 24 h after treatment. As expected, the overexpression of Spy1, Cyclin A and Cyclin E significantly increased cell numbers in the absence of any CKI (**Figure 7A**). Treatment with all CKIs in control cells resulted in a significant reduction in total live cells, whereas lower levels of response were seen in the presence of overexpressed Spy1, Cyclin A, and Cyclin E. The viability of Spy1 overexpressing cells depended on the cell line. MDA-MB-231 cells were least sensitive to roscovitine and most responsive to NU6201, while Cyclin A overexpressing cells were most sensitive to roscovitine and

least sensitive to purvalanol A. Cyclin E overexpressing cells were similar to Spy1 in that they were most sensitive to NU6201, however they demonstrated the least response to flavopiridol and CR8.
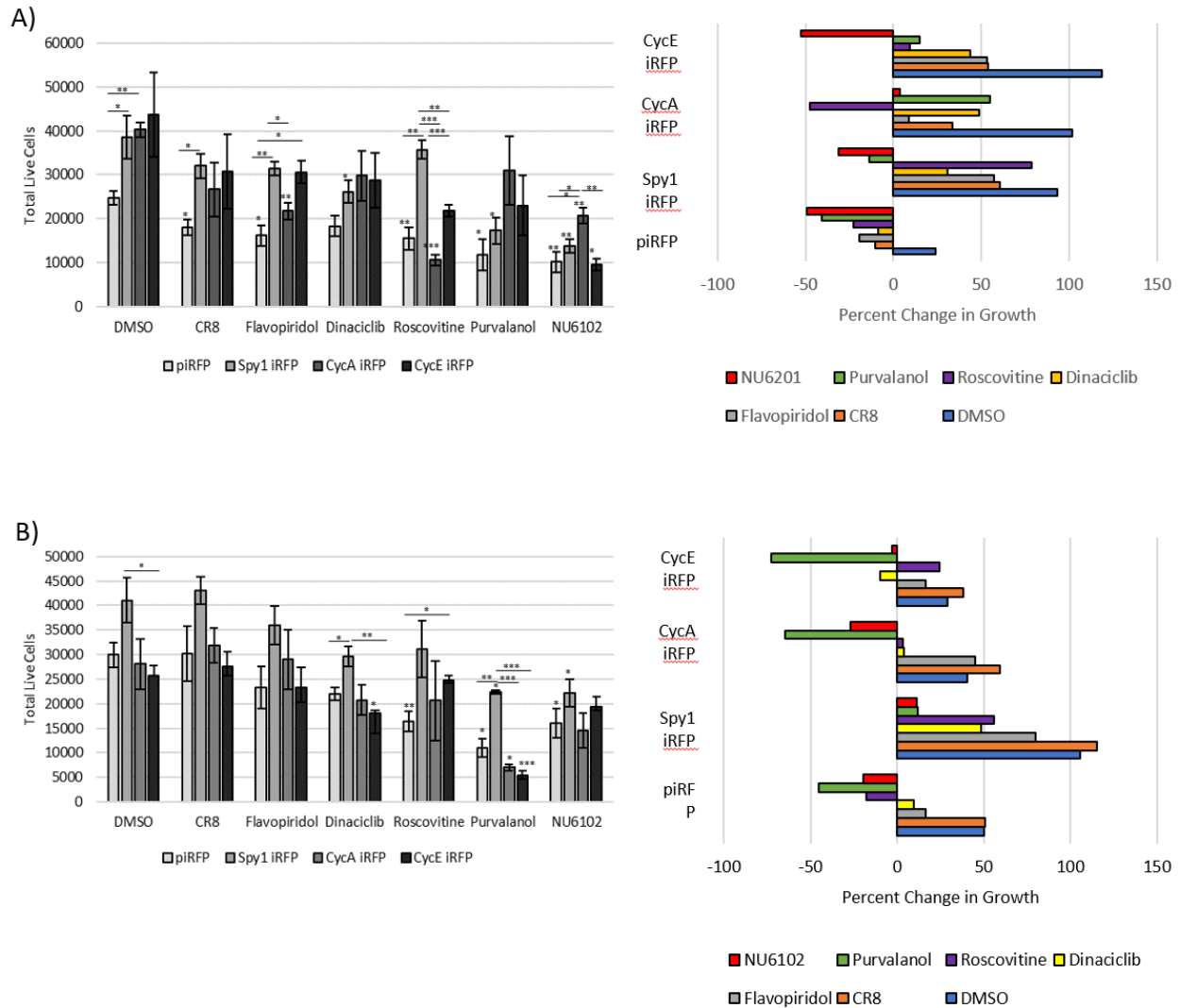
Figure 5 Spy1 increases resistance to CKI therapy. A) MDA-MB-231 and B) MDA-MB-468 cells were lentivirally infected with control (piRFP), Spy1 (Spy1 iRFP), Cyclin A (CycA iRFP) or Cyclin E (CycE iRFP) overexpression plasmids and treated with a panel of commercially available CKIs for 24hrs. Total number of live cells (left panels) were quantified *via* trypan blue exclusion assay. Percent change in growth from time of seeding is depicted on the right panels. Error bars reflect standard error (SE), Student's T test *p < 0.05, **p <0.01, ***p < 0.001.
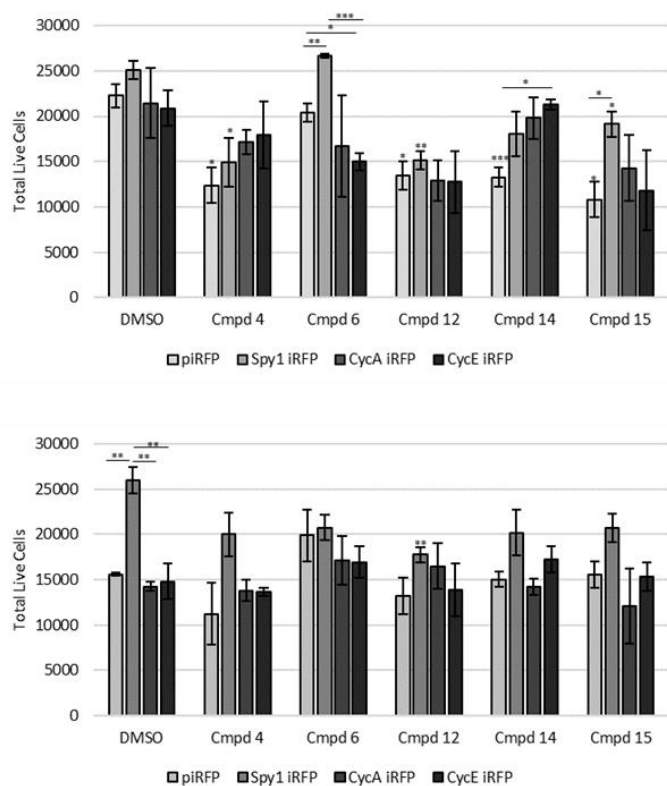
Figure 8. Differential response to NU series CDK inhibitors. A) MDA-MB-231 and B) MDA-MB-468 cells were lentivirally infected with control (piRFP), Spy1 (Spy1 iRFP), Cyclin A (CycA iRFP) or Cyclin E (CycE iRFP) overexpression plasmids and treated with a panel of NU series compounds for 24 hrs. Total number of live cells were quantified via trypan blue exclusion assay. Error bars reflect standard error (SE), Student's T test *p < 0.05, **p <0.01, ***p < 0.001.

In MDA-MB-468 cells, Spy1 overexpression was most responsive to NU6201, and purvalanol A, while being most resistant to CR8 (**Figure 7B**). Cyclin A and Cyclin E overexpression resulted in a similar response profile, being most responsive to purvalanol A and similar to Spy1, most resistant to CR8 (**Figure 7B**).

MDA-MB-231 and MDA-MB-468 cells, lentivirally transfected with one of Spy1, Cyclin A, or Cyclin E, were similarly treated with a panel of synthetic NU guanine-based inhibitors (**Figure 8**).[39] While varying responses were seen between the two cell lines, in almost all cases, the cells with Spy1 overexpression showed increased viability when treated (or untreated) compared to cells overexpressing any of the other cyclins. This is consistent with all our previous

studies that highlight how Spy1 drives proliferation. These NU series molecules are the previously reported molecules with the best known Spy1 inhibitory potential. They do, generally, show an ability to suppress cells overexpressing Spy1 by at least as much as cells overexpressing the other Cyclins; however, they are still only moderately effective, new drugs are needed.

Conclusion

We investigated whether the translational failure of CDK2 inhibitors could be a result of CDK2 activation by Spy1. Docking and MD/MM-GBSA methods showed good correlation with experimental data for Cyclin A-CDK2 and Cyclin E-CDK2 binding and was used to compare expected binding affinity between Spy1-CDK2 and Cyclin A-CDK2. In nearly all cases, compounds were predicted to bind significantly worse to Spy1-CDK2, caused by a change in active site structures. This sheds insight into why CDK2 inhibitors lack efficacy in treatment of aggressive or resistant cancers with elevated Spy1 expression. Our results show that the Spy1-CDK2 complex needs to be taken into account in the future development of CDK2 inhibitors as Spy1 induces a significant enough change in the active site to negatively impact CKI function.

Supporting Information

Additional Tables, including those showing the structures and computational parameters for the NU series molecules examined, are available in the SI.

Acknowledgements

Author Contributions

Conceptualization, JFT and LAP; Funding acquisition JFT and LP; Investigation, DM, JJH, and B-AF; Methodology, All authors ; Visualization, DM, B-AF; Project administration, JFT and LAP; Supervision, JFT and LAP; Writing original draft, DM and B-AF; Writing – review and editing, All authors.

References

1.   Malumbres, M., Cyclin-dependent kinases. *Genome Biol.* **2014,** *15* (6), 122.

2.   De Bondt, H. L.; Rosenblatt, J.; Jancarik, J.; Jones, H. D.; Morgan, D. O.; Kim, S.-H., Crystal structure of cyclin-dependent kinase 2. *Nature* **1993,** *363* (6430), 595-602.

3.   Blain, S. W.; Montalvo, E.; Massagué, J., Differential interaction of the cyclin-dependent kinase (CDK) inhibitor p27kip1 with cyclin A-CDK2 and cyclin D2-CDK4. *J. Biol. Chem.* **1997,** *272* (41), 25863-25872.

4.   (a) Ortega, S.; Malumbres, M.; Barbacid, M., Cyclin D-dependent kinases, INK4 inhibitors and cancer. *Biochim. Biophys. Acta.* **2002,** *1602* (1), 73-87; (b) Tadesse, S.; Anshabo, A. T.; Portman, N.; Lim, E.; Tilley, W.; Caldon, C. E.; Wang, S., Targeting CDK2 in cancer: Challenges and opportunities for therapy. *Drug Discov. Today* **2020,** *25* (2), 406-413.

5.   Peyressatre, M.; Prével, C.; Pellerano, M.; Morris, M. C., Targeting cyclin-dependent kinases in human cancers: From small molecules to peptide inhibitors. *Cancers (Basel)* **2015,** *7* (1), 179-237.

6.   Asghar, U.; Witkiewicz, A. K.; Turner, N. C.; Knudsen, E. S., The history and future of targeting cyclin-dependent kinases in cancer therapy. *Nat. Rev. Drug Discov.* **2015,** *14* (2), 130-146.

7.   Ortega, S.; Prieto, I.; Odajima, J.; Martin, A.; Dubus, P.; Sotillo, R.; Barbero, J. L.; Malumbres, M.; Barbacid, M., Cyclin-dependent kinase 2 is essential for meiosis but not for mitotic cell division in mice. *Nat. Genet.* **2003,** *35* (1), 25-31.

8.   (a) Horiuchi, D.; Kusdra, L.; Huskey, N. E.; Chandriani, S.; Lenburg, M. E.; Gonzalez-Angulo, A. M.; Creasman, K. J.; Bazarov, A. V.; Smyth, J. W.; Davis, S. E.; Yaswen, P.; Mills, G. B.; Esserman, L. J.; Goga, A., MYC pathway activation in triple-negative breast cancer is synthetic lethal with CDK inhibition. *J. Exp. Med.* **2012,** *209* (4), 679-96; (b) Molenaar, J. J.; Ebus, M. E.; Geerts, D.; Koster, J.; Lamers, F.; Valentijn, L. J.; Westerhout, E. M.; Versteeg, R.; Caron, H. N., Inactivation of CDK2 is synthetically lethal to MYCN over-expressing cancer cells. *Proc. Natl. Acad. Sci. U. S. A* **2009,** *106* (31), 12968-12973; (c) Cheng, C. K.; Gustafson, W. C.; Charron, E.; Houseman, B. T.; Zunder, E.; Goga, A.; Gray, N. S.; Pollok, B.; Oakes, S. A.; James, C. D.; Shokat, K. M.; Weiss, W. A.; Fan, Q.-W., Dual blockade of lipid and cyclin-dependent kinases induces synthetic lethality in malignant glioma. *Proceedings of the National Academy of Sciences* **2012,** *109* (31), 12722-12727.

9.   Diaz-Padilla, I.; Siu, L. L.; Duran, I., Cyclin-dependent kinase inhibitors as potential targeted anticancer agents. *Invest. New Drugs* **2009,** *27* (6), 586.

10.   Eggersmann, T. K.; Degenhardt, T.; Gluz, O.; Wuerstlein, R.; Harbeck, N., CDK4/6 inhibitors expand the therapeutic options in breast cancer: Palbociclib, ribociclib and abemaciclib. *BioDrugs* **2019,** *33* (2), 125-135.

11.   Al Sorkhy, M.; Fifield, B.-A.; Myers, D.; Porter, L. A., Direct interactions with both p27 and Cdk2 regulate Spy1-mediated proliferation *in vivo* and *in vitro*. *Cell Cycle* **2016**, *15* (1), 128-136.

12.   McGrath, D. A.; Fifield, B.-A.; Marceau, A. H.; Tripathi, S.; Porter, L. A.; Rubin, S. M., Structural basis of divergent cyclin-dependent kinase activation by Spy1/RINGO proteins. *EMBO J.* **2017**, *36* (15), 2251-2262.

13.   (a) Cheng, A.; Xiong, W.; Ferrell, J. E., Jr.; Solomon, M. J., Identification and comparative analysis of multiple mammalian Speedy/Ringo proteins. *Cell Cycle* **2005**, *4* (1), 155-65; (b) Dinarina, A.; Perez, L. H.; Davila, A.; Schwab, M.; Hunt, T.; Nebreda, A. R., Characterization of a new family of cyclin-dependent kinase activators. *Biochem. J.* **2005**, *386* (Pt 2), 349-55; (c) Lubanska, D.; Qemo, I.; Byrne, M.; Matthews, K. N.; Fifield, B. A.; Brown, J.; da Silva, E. F.; Porter, L. A., The cyclin-like protein SPY1 overrides reprogramming induced senescence through EZH2 mediated H3K27me3. *Stem Cells* **2021**, *39* (12), 1688-1700; (d) Gonzalez, L.; Domingo-Muelas, A.; Duart-Abadia, P.; Nuñez, M.; Mikolcevic, P.; Llonch, E.; Cubillos-Rojas, M.; Cánovas, B.; Forrow, S. M. A.; Morante-Redolat, J. M.; Fariñas, I.; Nebreda, A. R., The atypical CDK activator RingoA/Spy1 regulates exit from quiescence in neural stem cells. *iScience* **2023**, *26* (3), 106202; (e) Golipour, A.; Myers, D.; Seagroves, T.; Murphy, D.; Evan, G. I.; Donoghue, D. J.; Moorehead, R. A.; Porter, L. A., The Spy1/RINGO family represents a novel mechanism regulating mammary growth and tumorigenesis. *Cancer Res.* **2008**, *68* (10), 3591-3600; (f) Gastwirt, R. F.; McAndrew, C. W.; Donoghue, D. J., Speedy/RINGO regulation of CDKs in cell cycle, checkpoint activation and apoptosis. *Cell Cycle* **2007**, *6* (10), 1188-1193; (g) McAndrew, C. W.; Gastwirt, R. F.; Donoghue, D. J., The atypical CDK activator Spy1 regulates the intrinsic DNA damage response and is dependent upon p53 to inhibit apoptosis. *Cell Cycle* **2009**, *8* (1), 66-75.

14.   (a) Fifield, B. A.; Qemo, I.; Kirou, E.; Cardiff, R. D.; Porter, L. A., The atypical cyclin-like protein Spy1 overrides p53-mediated tumour suppression and promotes susceptibility to breast tumourigenesis. *Breast Cancer Res.* **2019**, *21* (1), 140; (b) Fifield, B. A.; Talia, J.; Stoyanovich, C.; Elliott, M. J.; Bakht, M. K.; Basilious, A.; Samsoondar, J. P.; Curtis, M.; Stringer, K. F.; Porter, L. A., Cyclin-like proteins tip regenerative balance in the liver to favour cancer formation. *Carcinogenesis* **2020**, *41* (6), 850-862.

15.   (a) Al Sorkhy, M.; Ferraiuolo, R.-M.; Jalili, E.; Malysa, A.; Fratiloiu, A. R.; Sloane, B. F.; Porter, L. A., The cyclin-like protein Spy1/RINGO promotes mammary transformation and is elevated in human breast cancer. *BMC Cancer* **2012**, *12* (1), 45; (b) Lu, S.; Liu, R.; Su, M.; Wei, Y.; Yang, S.; He, S.; Wang, X.; Qiang, F.; Chen, C.; Zhao, S.; Zhang, W.; Xu, P.; Mao, G., Spy1 participates in the proliferation and apoptosis of epithelial ovarian cancer. *J. Mol. Histol.* **2016**, *47* (1), 47-57; (c) Jin, Q.; Liu, G.; Bao, L.; Ma, Y.; Qi, H.; Yun, Z.; Dai, Y.; Zhang, S., High Spy1 expression predicts poor prognosis in colorectal cancer. *Cancer Manage. Res.* **2018**, *10*, 2757-2765; (d) Ke, Q.; Ji, J.; Cheng, C.; Zhang, Y.; Lu, M.; Wang, Y.; Zhang, L.; Li, P.; Cui, X.; Chen, L.; He, S.; Shen, A., Expression and prognostic role of Spy1 as a novel cell cycle protein in hepatocellular carcinoma. *Exp. Mol. Pathol.* **2009**, *87* (3), 167-72; (e) Zhang, L.; Shen, A.; Ke, Q.; Zhao, W.; Yan, M.; Cheng, C., Spy1 is frequently overexpressed in malignant gliomas and critically regulates the proliferation of glioma cells. *J. Mol. Neurosci.* **2012**, *47* (3), 485-94; (f) Lubanska, D.; Market-Velker, Brenna A.; deCarvalho, Ana C.; Mikkelsen, T.; Fidalgo da Silva, E.; Porter, Lisa A., The cyclin-like protein Spy1 regulates growth and division characteristics of the

CD133+ population in human glioma. *Cancer Cell* **2014,** *25* (1), 64-76; (g) Hang, Q.; Fei, M.; Hou, S.; Ni, Q.; Lu, C.; Zhang, G.; Gong, P.; Guan, C.; Huang, X.; He, S., Expression of Spy1 protein in human non-Hodgkin's lymphomas is correlated with phosphorylation of p27 Kip1 on Thr187 and cell proliferation. *Med. Oncol.* **2012,** *29* (5), 3504-14.

16.   (a) Ferraiuolo, R.-M.; Tubman, J.; Sinha, I.; Hamm, C.; Porter, L. A., The cyclin-like protein, SPY1, regulates the ERα and ERK1/2 pathways promoting tamoxifen resistance. *Oncotarget* **2017,** *8* (14), 23337-23352; (b) Barnes, E. A.; Porter, L. A.; Lenormand, J.-L.; Dellinger, R. W.; Donoghue, D. J., Human Spy1 promotes survival of mammalian cells following DNA damage. *Cancer Res.* **2003,** *63* (13), 3701-3707; (c) Ferraiuolo, R.-M.; Fifield, B.-A.; Hamm, C.; Porter, L. A., Stabilization of c-Myc by the atypical cell cycle regulator, Spy1, decreases efficacy of breast cancer treatments. *Breast Cancer Res. Treat.* **2022,** *196* (1), 17-30.

17.   (a) Gonzalez, L.; Nebreda, A. R., RINGO/Speedy proteins, a family of non-canonical activators of CDK1 and CDK2. *Semin. Cell Dev. Biol.* **2020,** *107*, 21-27; (b) Mikolcevic, P.; Isoda, M.; Shibuya, H.; del Barco Barrantes, I.; Igea, A.; Suja, J. A.; Shackleton, S.; Watanabe, Y.; Nebreda, A. R., Essential role of the Cdk2 activator RingoA in meiotic telomere tethering to the nuclear envelope. *Nat. Commun.* **2016,** *7*, 11084; (c) Tu, Z.; Bayazit, M. B.; Liu, H.; Zhang, J.; Busayavalasa, K.; Risal, S.; Shao, J.; Satyanarayana, A.; Coppola, V.; Tessarollo, L.; Singh, M.; Zheng, C.; Han, C.; Chen, Z.; Kaldis, P.; Gustafsson, J. A.; Liu, K., Speedy A-Cdk2 binding mediates initial telomere-nuclear envelope attachment during meiotic prophase I independent of Cdk2 activation. *Proc. Natl. Acad. Sci. U. S. A.* **2017,** *114* (3), 592-597.

18.   (a) Faber, E. B.; Sun, L.; Tang, J.; Roberts, E.; Ganeshkumar, S.; Wang, N.; Rasmussen, D.; Majumdar, A.; Hirsch, L. E.; John, K.; Yang, A.; Khalid, H.; Hawkinson, J. E.; Levinson, N. M.; Chennathukuzhi, V.; Harki, D. A.; Schönbrunn, E.; Georg, G. I., Development of allosteric and selective CDK2 inhibitors for contraception with negative cooperativity to cyclin binding. *Nat. Commun.* **2023,** *14* (1), 3213; (b) Faber, E. B.; Wang, N.; John, K.; Sun, L.; Wong, H. L.; Burban, D.; Francis, R.; Tian, D.; Hong, K. H.; Yang, A.; Wang, L.; Elsaid, M.; Khalid, H.; Levinson, N. M.; Schönbrunn, E.; Hawkinson, J. E.; Georg, G. I., Screening through lead optimization of high affinity, allosteric cyclin-dependent kinase 2 (CDK2) inhibitors as male contraceptives that reduce sperm counts in mice. *J. Med. Chem.* **2023,** *66* (3), 1928-1940.

19.   (a) Gibson, A. E.; Arris, C. E.; Bentley, J.; Boyle, F. T.; Curtin, N. J.; Davies, T. G.; Endicott, J. A.; Golding, B. T.; Grant, S.; Griffin, R. J.; Jewsbury, P.; Johnson, L. N.; Mesguiche, V.; Newell, D. R.; Noble, M. E. M.; Tucker, J. A.; Whitfield, H. J., Probing the ATP ribose-binding domain of cyclin-dependent kinases 1 and 2 with O6-substituted guanine derivatives. *J. Med. Chem.* **2002,** *45* (16), 3381-3393; (b) Hardcastle, I. R.; Arris, C. E.; Bentley, J.; Boyle, F. T.; Chen, Y.; Curtin, N. J.; Endicott, J. A.; Gibson, A. E.; Golding, B. T.; Griffin, R. J.; Jewsbury, P.; Menyerol, J.; Mesguiche, V.; Newell, D. R.; Noble, M. E. M.; Pratt, D. J.; Wang, L.-Z.; Whitfield, H. J., N2-Substituted O6-cyclohexylmethylguanine derivatives: Potent inhibitors of cyclin-dependent kinases 1 and 2. *J. Med. Chem.* **2004,** *47* (15), 3710-3722; (c) Griffin, R. J.; Henderson, A.; Curtin, N. J.; Echalier, A.; Endicott, J. A.; Hardcastle, I. R.; Newell, D. R.; Noble, M. E. M.; Wang, L.-Z.; Golding, B. T., Searching for cyclin-dependent kinase inhibitors using a new variant of the Cope elimination. *J. Am. Chem. Soc* **2006,** *128* (18), 6012-6013; (d) Coxon, C. R.; Anscombe, E.; Harnor, S. J.; Martin, M. P.; Carbain, B.; Golding, B. T.; Hardcastle, I. R.; Harlow, L. K.; Korolchuk, S.; Matheson, C. J.; Newell, D. R.; Noble, M. E. M.; Sivaprakasam, M.;

Tudhope, S. J.; Turner, D. M.; Wang, L. Z.; Wedge, S. R.; Wong, C.; Griffin, R. J.; Endicott, J. A.; Cano, C., Cyclin-dependent kinase (CDK) inhibitors: Structure–activity relationships and insights into the CDK-2 selectivity of 6-substituted 2-arylaminopurines. *J. Med. Chem.* **2017,** *60* (5), 1746-1767.

20.   (a) K. Lembicz, N.; Grant, S.; Clegg, W.; J. Griffin, R.; L. Heath, S.; T. Golding, B., Facilitation of displacements at the 6-position of purines by the use of 1,4-diazabicyclo[2.2.2]octane as leaving group. *J. Chem. Soc. Perk. Trans. 1* **1997,** (3), 185-186; (b) Arris, C. E.; Boyle, F. T.; Calvert, A. H.; Curtin, N. J.; Endicott, J. A.; Garman, E. F.; Gibson, A. E.; Golding, B. T.; Grant, S.; Griffin, R. J.; Jewsbury, P.; Johnson, L. N.; Lawrie, A. M.; Newell, D. R.; Noble, M. E. M.; Sausville, E. A.; Schultz, R.; Yu, W., Identification of novel purine and pyrimidine cyclin-dependent kinase inhibitors with distinct molecular interactions and tumor cell growth inhibition profiles. *J. Med. Chem.* **2000,** *43* (15), 2797-2804; (c) Davies, T. G.; Bentley, J.; Arris, C. E.; Boyle, F. T.; Curtin, N. J.; Endicott, J. A.; Gibson, A. E.; Golding, B. T.; Griffin, R. J.; Hardcastle, I. R.; Jewsbury, P.; Johnson, L. N.; Mesguiche, V.; Newell, D. R.; Noble, M. E. M.; Tucker, J. A.; Wang, L.; Whitfield, H. J., Structure-based design of a potent purine-based cyclin-dependent kinase inhibitor. *Nat. Struct. Biol.* **2002,** *9*, 745; (d) Whitfield, H. J.; Griffin, R. J.; Hardcastle, I. R.; Henderson, A.; Meneyrol, J.; Mesguiche, V.; Sayle, K. L.; Golding, B. T., Facilitation of addition–elimination reactions in pyrimidines and purines using trifluoroacetic acid in trifluoroethanol. *Chem. Commun.* **2003,** (22), 2802-2803.

21.   Citti, C.; Linciano, P.; Russo, F.; Luongo, L.; Iannotta, M.; Maione, S.; Laganà, A.; Capriotti, A. L.; Forni, F.; Vandelli, M. A.; Gigli, G.; Cannazza, G., A novel phytocannabinoid isolated from *Cannabis sativa L.* with an *in vivo* cannabimimetic activity higher than Δ9-tetrahydrocannabinol: Δ9-Tetrahydrocannabiphorol. *Sci. Rep.* **2019,** *9* (1), 20335.

22.   Chen, P.; Lee, N. V.; Hu, W.; Xu, M.; Ferre, R. A.; Lam, H.; Bergqvist, S.; Solowiej, J.; Diehl, W.; He, Y.-A.; Yu, X.; Nagata, A.; VanArsdale, T.; Murray, B. W., Spectrum and degree of CDK drug interactions predicts clinical performance. *Mol. Cancer Ther.* **2016,** *15* (10), 2273-2281.

23.   Protein Data Bank. [http://www.rcsb.org/pdb].

24.   Madhavi Sastry, G.; Adzhigirey, M.; Day, T.; Annabhimoju, R.; Sherman, W., Protein and ligand preparation: Parameters, protocols, and influence on virtual screening enrichments. *J. Comput. -Aided Mol. Des.* **2013,** *27* (3), 221-234.

25.   *LigPrep 2019-03*, Schrödinger: New York, NY,, 2019.

26.   (a) Friesner, R. A.; Murphy, R. B.; Repasky, M. P.; Frye, L. L.; Greenwood, J. R.; Halgren, T. A.; Sanschagrin, P. C.; Mainz, D. T., Extra precision Glide: Docking and scoring incorporating a model of hydrophobic enclosure for protein−ligand complexes. *J. Med. Chem.* **2006,** *49* (21), 6177-6196; (b) Sherman, W.; Day, T.; Jacobson, M. P.; Friesner, R. A.; Farid, R., Novel procedure for modeling ligand/receptor induced fit effects. *J. Med. Chem.* **2006,** *49* (2), 534-553.
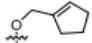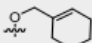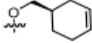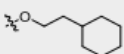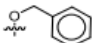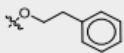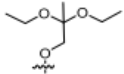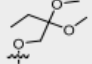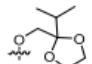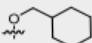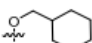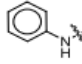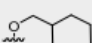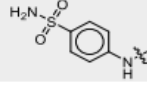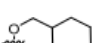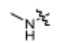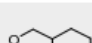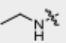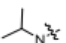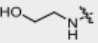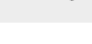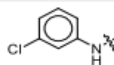
27.   Li, J.; Abel, R.; Zhu, K.; Cao, Y.; Zhao, S.; Friesner, R. A., The VSGB 2.0 model: A next generation energy model for high resolution protein structure modeling. *Protein Struct. Funct. Bioinf.* **2011,** *79* (10), 2794-2812.

28.   Lu, C.; Wu, C.; Ghoreishi, D.; Chen, W.; Wang, L.; Damm, W.; Ross, G. A.; Dahlgren, M. K.; Russell, E.; Von Bargen, C. D.; Abel, R.; Friesner, R. A.; Harder, E. D., OPLS4: Improving force field accuracy on challenging regimes of chemical space. *J. Chem. Theory Comput.* **2021,** *17* (7), 4291-4300.

29.   Case, D. A.; Aktulga, H. M.; Belfon, K.; Ben-Shalom, I. Y.; Brozell, S. R.; Cerutti, D. S.; Cheatham, T. E.; Cisneros, G. A.; Cruzeiro, V. W. D.; Darden, T. A.; Duke, R. E.; Giambasu, G.; Gilson, M. K.; Gohlke, H.; Goetz, A. W.; Harris, R.; Izadi, S.; Izmailov, S. A.; Jin, C.; Kasavajhala, K.; Kaymak, M. C.; King, E.; Kovalenko, A.; Kurtzman, T.; Lee, T. S.; LeGrand, S.; Li, P.; Lin, C.; Liu, J.; Luchko, T.; Luo, R.; Machado, M.; Man, V.; Manathunga, M.; Merz, K. M.; Miao, Y.; Mikhailovskii, O.; Monard, G.; Nguyen, H.; O'Hearn, K. A.; Onufriev, A.; Pan, F.; Pantano, S.; Qi, R.; Rahnamoun, A.; Roe, D. R.; Roitberg, A.; Sagui, C.; Schott-Verdugo, S.; Shen, J.; Simmerling, C. L.; Skrynnikov, N. R.; Smith, J.; Swails, J.; Walker, R. C.; Wang, J.; Wei, H.; Wolf, R. M.; Wu, X.; Xue, Y.; York, D. M.; Zhao, S.; Kollman, P. A. *Amber 2021*, University of California, San Francisco, 2021.

30.   (a) Bayly, C. I.; Cieplak, P.; Cornell, W.; Kollman, P. A., A well-behaved electrostatic potential based method using charge restraints for deriving atomic charges: The RESP model. *J. Phys. Chem.* **1993,** *97* (40), 10269-10280; (b) Cornell, W. D.; Cieplak, P.; Bayly, C. I.; Kollman, P. A., Application of RESP charges to calculate conformational energies, hydrogen bond energies, and free energies of solvation. *J. Am. Chem. Soc.* **1993,** *115* (21), 9620-9631.

31.   Frisch, M. J.; Trucks, G. W.; Schlegel, H. B.; Scuseria, G. E.; Robb, M. A.; Cheeseman, J. R.; Scalmani, G.; Barone, V.; Petersson, G. A.; Nakatsuji, H.; Li, X.; Caricato, M.; Marenich, A. V.; Bloino, J.; Janesko, B. G.; Gomperts, R.; Mennucci, B.; Hratchian, H. P.; Ortiz, J. V.; Izmaylov, A. F.; Sonnenberg, J. L.; Williams; Ding, F.; Lipparini, F.; Egidi, F.; Goings, J.; Peng, B.; Petrone, A.; Henderson, T.; Ranasinghe, D.; Zakrzewski, V. G.; Gao, J.; Rega, N.; Zheng, G.; Liang, W.; Hada, M.; Ehara, M.; Toyota, K.; Fukuda, R.; Hasegawa, J.; Ishida, M.; Nakajima, T.; Honda, Y.; Kitao, O.; Nakai, H.; Vreven, T.; Throssell, K.; Montgomery Jr., J. A.; Peralta, J. E.; Ogliaro, F.; Bearpark, M. J.; Heyd, J. J.; Brothers, E. N.; Kudin, K. N.; Staroverov, V. N.; Keith, T. A.; Kobayashi, R.; Normand, J.; Raghavachari, K.; Rendell, A. P.; Burant, J. C.; Iyengar, S. S.; Tomasi, J.; Cossi, M.; Millam, J. M.; Klene, M.; Adamo, C.; Cammi, R.; Ochterski, J. W.; Martin, R. L.; Morokuma, K.; Farkas, O.; Foresman, J. B.; Fox, D. J. *Gaussian 16 Rev. C.01*, Wallingford, CT, 2016.

32.   Wang, J.; Wang, W.; Kollman, P. A.; Case, D. A., Automatic atom type and bond type perception in molecular mechanical calculations. *J. Mol. Graphics Modell.* **2006,** *25* (2), 247-260.

33.   Xu, L.; Sun, H.; Li, Y.; Wang, J.; Hou, T., Assessing the performance of MM/PBSA and MM/GBSA methods. 3. The impact of force fields and ligand charge models. *J. Phys. Chem. B* **2013,** *117* (28), 8408-8421.

34.   (a) Jakalian, A.; Bush, B. L.; Jack, D. B.; Bayly, C. I., Fast, efficient generation of high-quality atomic charges. AM1-BCC model: I. Method. *J. Comput. Chem.* **2000,** *21* (2), 132-146; (b) Jakalian, A.; Jack, D. B.; Bayly, C. I., Fast, efficient generation of high-quality atomic charges. AM1-BCC model: II. Parameterization and validation. *J. Comput. Chem.* **2002,** *23* (16), 1623-1641.

35.   Wang, J.; Wolf, R. M.; Caldwell, J. W.; Kollman, P. A.; Case, D. A., Development and testing of a general Amber force field. *J. Comput. Chem.* **2004,** *25* (9), 1157-1174.

36.   Maier, J. A.; Martinez, C.; Kasavajhala, K.; Wickstrom, L.; Hauser, K. E.; Simmerling, C., ff14SB: Improving the accuracy of protein side chain and backbone parameters from ff99SB. *J. Chem. Theory Comput.* **2015,** *11* (8), 3696-3713.

37.   Jorgensen, W. L.; Chandrasekhar, J.; Madura, J. D.; Impey, R. W.; Klein, M. L., Comparison of simple potential functions for simulating liquid water. *J. Chem. Phys.* **1983,** *79* (2), 926-935.

38.   Russo, A. A.; Jeffrey, P. D.; Pavletich, N. P., Structural basis of cyclin-dependent kinase activation by phosphorylation. *Nat. Struct. Biol.* **1996,** *3* (8), 696-700.

39.   Mader, L.; Hayward, J. J.; Porter, L. A.; Trant, J., F., A revised synthesis of 6-alkoxy-2-aminopurines with late-stage convergence allowing for increased molecular complexity. *New J. Chem.* **2022,** *46*, 17040-17048.

Table S3 Structure of NU compounds and experimental inhibition of Cyclin A-CDK2 and Cyc B-CDK2 and docking scores for the compounds docked to Cyclin-CDK or Spy1-CDK2 complexes.

Compound	R1	R2	Cdk2/CycA Inhibition (IC$_{50}$ μM)	Cdk1/CycB Inhibition (IC$_{50}$ μM)	CDK2/Cyclin A Dock Score	CDK2/Cyclin E Dock Score	CDK1/Cyclin B Dock Score	CDK2/Spy1 Dock Score
1		NH$_2$	67.00	75.00	-8.74	-7.14	-8.29	-5.00
2		NH$_2$	48.00	32.00	-8.49	-7.90	-8.09	-5.18
3		NH$_2$	49.00	37.00	-8.87	-8.02	-8.35	-5.04
4		NH$_2$	75.00	75.00	-8.27	-6.90	-8.27	-5.61
5		NH$_2$	25.00	27.00	-8.04	-6.45	-7.39	-6.29
6		NH$_2$	42.00	45.00	-8.68	-8.07	-8.38	-5.88
7		NH$_2$	15.00	17.00	-8.43	-8.34	-8.19	-5.32
8		NH$_2$	26.00	21.00	-8.79	-7.46	-8.41	-5.17
9		NH$_2$	90.00	91.00	-8.73	-7.00	-8.13	-3.75
10		NH$_2$	47.00	41.00	-8.74	-7.51	-7.41	-4.20
11		NH$_2$	69.00	76.00	-9.14	-8.55	-8.17	-4.80
12		NH$_2$	78.00	68.00	-8.56	-6.78	-7.89	-4.21
13		NH$_2$	35.00	32.00	-8.67	-6.98	-8.18	-4.84
14		NH$_2$	21.00	19.00	-8.91	-7.91	-8.46	-5.22
15		NH$_2$	16.00	11.00	-9.14	-7.93	-8.48	-5.65
16		NH$_2$	34.00	25.00	-10.34	-9.90	-9.13	-4.94
17		NH$_2$	21.00	15.00	-9.23	-8.07	-9.05	-4.37

Compound	R1	R2	Cdk2/CycA Inhibition (IC$_{50}$ μM)	Cdk1/CycB Inhibition (IC$_{50}$ μM)	CDK2/Cyclin A Dock Score	CDK2/Cyclin E Dock Score	CDK1/Cyclin B Dock Score	CDK2/Spy1 Dock Score
18		NH$_2$	31.00	19.00	-9.20	-7.66	-8.82	-5.81
19		NH$_2$	22.00	11.00	-9.68	-8.07	-9.24	-5.98
20		NH$_2$	16.00	6.00	-9.15	-8.79	-8.83	-7.27
21		NH$_2$	44.00	37.00	-9.80	-6.77	-9.17	-5.87
22		NH$_2$	35.00	24.00	-9.66	-8.20	-8.43	-5.72
23		NH$_2$	65.00	59.00	-10.22	-8.73	-8.98	-6.16
24		NH$_2$	33.00	36.00	-9.61	-8.59	-9.04	-5.97
25		NH$_2$	20.00	19.00	-8.62	-6.95	-7.85	-5.50
26		NH$_2$	65.00	39.00	-8.92	-6.96	-7.25	-5.60
27		NH$_2$	17.00	7.00	-9.66	-9.20	-8.91	-5.89
28			0.97	1.60	-10.79	-9.97	-9.64	-7.67
29			0.0054		-12.11	-9.96	-10.74	-8.72
30			5.00	5.30	-9.46	-9.61	-8.69	-7.31
31			2.80	3.30	-9.85	-9.54	-8.42	-7.45
32			1.20	2.00	-10.10	-10.06	-9.20	-7.71
33			2.80	3.20	-9.74	-9.43	-8.88	-6.60
34			2.30	2.20	-10.73	-9.83	-9.66	-8.01

Compound	R1	R2	Cdk2/CycA Inhibition (IC$_{50}$ μM)	Cdk1/CycB Inhibition (IC$_{50}$ μM)	CDK2/Cyclin A Dock Score	CDK2/Cyclin E Dock Score	CDK1/Cyclin B Dock Score	CDK2/Spy1 Dock Score
35			6.80	5.30	-10.81	-9.60	-9.20	-7.78
36			12.00	13.00	-10.23	-9.84	-8.90	-7.89
37			0.40	0.30	-11.94	-9.35	-10.53	-8.01
38			1.80	2.20	-10.54	-9.19	-9.02	-7.48
39			1.70	2.40	-10.51	-10.02	-8.36	-7.56
40			0.07	0.09	-10.96	-10.22	-10.13	-8.46
41			0.65	0.79	-10.47	-10.01	-9.19	-7.66
42			0.01	0.01	-11.73	-8.95	-10.36	-7.78
43			0.06	0.08	-11.15	-6.20	-9.84	-7.90
44			0.06	0.08	-11.32	-9.62	-10.11	-7.82
45			0.10	0.20	-11.82	-8.87	-10.64	-8.28
46			0.07	0.10	-12.01	-9.87	-10.25	-7.13
47			0.21	0.24	-11.58	-10.30	-9.07	-8.31
48			0.06	0.07	-11.27	-10.07	-10.51	-6.56
49			0.20	0.40	-10.92	-9.49	-9.89	-7.98
50			0.20	0.60	-10.99	-8.31	-9.64	-7.60
51			0.30	0.50	-11.39	-9.47	-9.69	-7.79

Compound	R1	R2	Cdk2/CycA Inhibition (IC$_{50}$ µM)	Cdk1/CycB Inhibition (IC$_{50}$ µM)	CDK2/Cyclin A Dock Score	CDK2/Cyclin E Dock Score	CDK1/Cyclin B Dock Score	CDK2/Spy1 Dock Score
52			0.80	1.00	-11.28	-10.25	-9.10	-8.19
53			0.13	0.14	-11.27	-10.07	-10.51	-6.56
54			0.30	0.30	-11.50	-9.24	-9.93	-7.64
55			1.70	0.70	-9.68	-9.98	-9.09	-7.67
56			5.00	5.70	-10.29	-11.12	-9.53	-8.57
57			4.30	n/a	8.90	-8.96	-5.63	-7.53
58			0.16	n/a	-11.35	-10.09	-10.04	-7.36
59			0.12	6.30	-11.84	-9.91	-10.16	-10.37
60			0.34	n/a	-9.65	-10.32	-10.46	-6.08
61			0.54	n/a	-11.24	-10.05	-10.08	-7.68
62			0.45	n/a	-10.05	-9.99	-9.94	-5.95
63			0.45	n/a	-11.01	-9.84	-9.57	-7.67
64			0.05	1.60	-12.78	-10.84	-11.20	-8.09
65			0.05	n/a	-11.41	-11.21	-10.79	-6.78
66			0.02	n/a	-8.64	-9.60	-10.35	-5.11
67			3.70	n/a	-9.30	-8.37	-9.92	-6.03
68			0.08	n/a	-10.31	-6.99	-11.37	-8.08
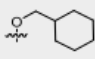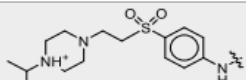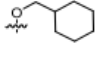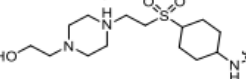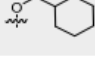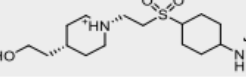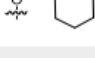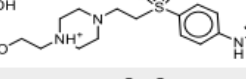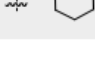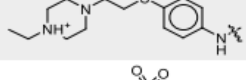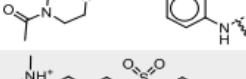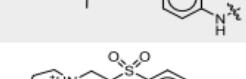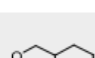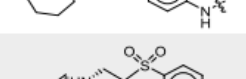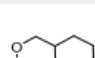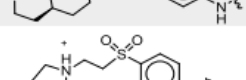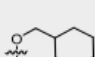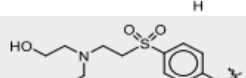
Compound	R1	R2	Cdk2/CycA Inhibition (IC$_{50}$ µM)	Cdk1/CycB Inhibition (IC$_{50}$ µM)	CDK2/Cyclin A Dock Score	CDK2/Cyclin E Dock Score	CDK1/Cyclin B Dock Score	CDK2/Spy1 Dock Score
69			0.34	5.60	-11.78	-6.34	-9.85	-8.84
70			0.26	3.40	-12.57	-10.57	-10.97	-7.80
71			0.24	2.80	-13.07	-9.61	-10.68	-7.95
72			0.31	2.20	-11.04	-8.68		
73			0.26	2.80	-11.79	-8.23	-9.46	-9.68
74			0.23	1.80	-11.65	-10.05	-10.14	-7.58
75			0.25	1.50	-11.60	-7.14	-10.43	-5.82
76			1.78	10.00	-11.08	-9.37	-9.97	-4.38
77			0.29	4.60	-12.02	-9.77	-10.57	-7.22
78			0.18	2.90	-12.09	-9.85	-10.61	-7.39
79			0.11	2.20	-10.95	-10.19	-9.48	-5.56

Table S4 Comparison of binding affinities obtained from MD-MM-GBSA. Values are averages of three independent simulations.

Cmpd.	CycA-CDK2 Binding Affinity	Spy1-CDK2 Binding Affinity	ΔBinding Affinity	Cmpd.	CycA-CDK2 Binding Affinity	Spy1-CDK2 Binding Affinity	ΔBinding Affinity
1	-27.33	-22.51	-4.81	44	-45.63	-36.88	-8.75
2	-27.56	-24.67	-2.89	45	-44.80	-38.30	-6.51
3	-30.46	-28.73	-1.73	46	-51.27	-36.85	-14.42
4	-27.75	-21.45	-6.29	47	-47.90	-36.43	-11.48
5	-28.71	-25.00	-3.71	48	-45.34	-40.01	-5.33
6	-29.15	-22.59	-6.56	49	-45.74	-43.71	-2.03
7	-30.56	-23.44	-7.11	50	-46.79	-42.43	-4.36
8	-30.57	-23.49	-7.08	51	-43.48	-37.67	-5.81
9	-26.56	-25.62	-0.94	52	-44.19	-35.22	-8.97
10	-32.93	-26.02	-6.91	53	-44.80	-37.89	-6.91
11	-32.54	-26.42	-6.12	54	-46.74	-39.45	-7.29
12	-25.32	-19.58	-5.74	55	-41.29	-37.22	-4.07
13	-28.13	-30.27	2.13	56	-44.18	-39.24	-4.95
14	-30.16	-24.45	-5.72	57	-42.79	-35.93	-6.87
15	-30.82	-25.90	-4.92	58	-47.39	-49.55	2.16
16	-38.61	-37.12	-1.49	59	-59.59	-39.40	-20.20
17	-31.71	-30.45	-1.26	60	-49.87	-44.16	-5.71
18	-30.74	-28.02	-2.72	61	-48.73	-47.04	-1.69
19	-32.22	-27.96	-4.26	62	-48.08	-45.44	-2.63
20	-30.59	-27.81	-2.79	63	-52.25	-45.34	-6.91
21	-31.90	-27.03	-4.86	64	-48.35	-42.05	-6.30
22	-30.65	-26.97	-3.68	65	-58.35	-45.87	-12.49
23	-31.57	-27.42	-4.16	66	-48.90	-44.75	-4.15
24	-36.05	-27.12	-8.92	67	-49.95	-46.79	-3.16
25	-32.70	-28.76	-3.94	68	-49.39	-44.96	-4.43
26	-33.61	-26.31	-7.30	69	-49.83	-40.54	-9.29
27	-32.86	-27.34	-5.52	70	-61.03	-40.10	-20.93
28	-43.36	-36.23	-7.13	71	-50.15	-37.74	-12.41
29	-46.36	-42.01	-4.35	72	-67.94	-60.71	-7.23
30	-35.56	-29.17	-6.40	73	-45.44	-42.07	-3.37
31	-39.05	-31.66	-7.39	74	-50.40	-41.02	-9.38
32	-39.64	-32.72	-6.93	75	-46.90	-38.73	-8.17
33	-43.33	-33.87	-9.46	76	-50.96	-25.77	-25.18
34	-44.58	-37.11	-7.48	77	-49.65	-41.55	-8.09
35	-45.43	-37.31	-8.12	78	-47.37	-35.74	-11.63
36	-44.82	-39.70	-5.11	79	-51.89	-41.63	-10.26
37	-46.14	-36.97	-9.18	Cr8 (A)	-43.66	-41.43	-2.23

38	-43.74	-35.00	-8.74	Cr8 (B)	-45.79	-42.83	-2.95
39	-44.67	-36.25	-8.42	Dinaciclib	-49.21	-45.90	-3.31
40	-46.94	-39.25	-7.69	flavopiridol	-42.68	-35.60	-7.09
41	-45.42	-38.21	-7.21	Purvalanol A	-43.35	-41.73	-1.62
42	-47.13	-42.27	-4.86	Roscovitine A	-39.32	-43.25	3.93
43	-48.15	-40.94	-7.21				